

The many surface expressions of mantle dynamics

Jean Braun

Plate tectonic theory suggests that present-day topography can be explained by the repeated interactions between the tectonic plates moving along Earth's surface. However, mounting evidence indicates that a significant proportion of Earth's topography results from the viscous stresses created by flow within the underlying mantle, rather than by the moving plates. This dynamic topography is transient, varying as mantle flow changes, and is characterized by small amplitudes and long wavelengths. It is therefore often hidden by or confused with the more obvious topographic anomalies resulting from horizontal tectonic movements. However, dynamic topography can influence surface processes and thus enter the geological record; it has, for example, played a role in the establishment of Amazon drainage patterns. In turn, surface processes such as the erosion of topographical anomalies could affect mantle flow. This emerging view of dynamic topography suggests that the concept of plate tectonics as the driver of surface deformation needs to be extended to include the vertical coupling between the mantle and the surface. Unravelling this coupling back in time with the help of models and the geological record can potentially provide unprecedented insights into past mantle dynamics.

Density variations in the Earth's mantle give rise to vigorous flow that interacts with the Earth's surface to create dynamic topography¹. Where mantle material rises or falls in the presence of the Earth's surface, the ensuing flow is strongly perturbed by the existence of this boundary, which acts as a quasi-undeformable obstacle (Fig. 1a). The interaction between the mantle flow and the surface boundary generates viscous stresses that are themselves balanced by the gravitational stresses arising from the vertical deflection of the surface (Fig. 1b): upward, divergent flow towards the surface leads to positive topography, whereas downward, convergent flow away from the surface leads to negative topography (surface depression). The height of dynamic topography is in direct proportion to the intensity and depth of mantle flow, and the wavelength of dynamic topography is proportional to the scale and depth of the flow. Interestingly, the core–mantle boundary, which forms another boundary at the base of the mantle, is also affected by dynamic topography¹.

Most of the Earth's present-day surface topography has been created by crustal and lithospheric thickness variations, resulting from horizontal tectonic plate motions (Fig. 1b). Because dynamic topography is transient and characterized by relatively low amplitudes and long wavelengths, it is often hidden by or confused with the topography created by horizontal tectonic movements. Therefore, the most direct way to estimate present-day dynamic topography is to subtract the component that is tectonic in origin — and associated with crustal and lithospheric thickness variations — from today's surface topography, by making use of local isostasy. According to the principle of isostasy, the lithosphere (the rigid 100-km-thick outer shell of the Earth) floats on the underlying less viscous asthenosphere or upper mantle, like an iceberg floats in the ocean; the thicker the iceberg, the higher its height above the water line. The remainder of topography — left over once the tectonically formed topography has been subtracted — is commonly accepted to be dynamically sustained by mantle flow. This dynamic topography is also known as residual topography^{2–6} and is characterized by a maximum amplitude of 1,000 m and a wavelength of several hundred to several thousand kilometres (Fig. 2a).

Maps of dynamic topography remain approximate, because our knowledge of crustal-thickness variations beneath the continents and the thermal structure, and thus thickness, of the lithosphere is not perfect. For example, the debate on why old ocean bathymetry flattens and deviates from a simple cooling half-space model still continues^{7,8}. Questions exist on how to accurately correct ocean bathymetry for the effect of sediment loading and the thermal-blanketing effect created by sediments at heavily sedimented passive margins⁹. Both corrections are crucial to compute the isostatically compensated topography component in old oceanic crust or near passive continental margins.

Present-day dynamic topography can also be computed from estimates of the mantle density structure derived from seismic tomography. Combined with our knowledge of mantle-rock viscosity, these can be used to compute the present-day pattern of mantle flow from which an independent estimate of the distribution (the wavelength and amplitude) of the present-day dynamic topography can be derived. One such recent estimate¹⁰ for the Earth's oceanic areas (Fig. 2b) and the spectrum of this computed dynamic topography (the distribution of its amplitude as a function of wavelength; Fig. 2c) show that, on a global scale, dynamic topography is also characterized by a maximum amplitude of 1,000 m and wavelengths of a few hundred to a few thousand kilometres. These surface characteristics are set by the amplitude and size of density anomalies in the mantle (imaged by seismic tomography), and by the filtering effect of the relatively rigid or high-viscosity lithosphere. At this stage, it is also worth noting that, unlike isostatically compensated topography, dynamic topography is transient, rising and moving with mantle flow. However, the rate of change of dynamic topography is relatively low (of the order of a few tens of metres per million years (Myr), as determined from mantle-flow models; Fig. 2b), and is set by the rate of change of mantle flow in the vicinity of the surface and the relative motion of lithospheric plates with respect to the underlying mantle.

In parallel with global estimates, much work has been devoted to characterizing dynamic topography in a variety of locations and settings. Mantle-flow-driven subsidence in subduction zones was first proposed to explain the 1,000-km-wavelength tilting of continents

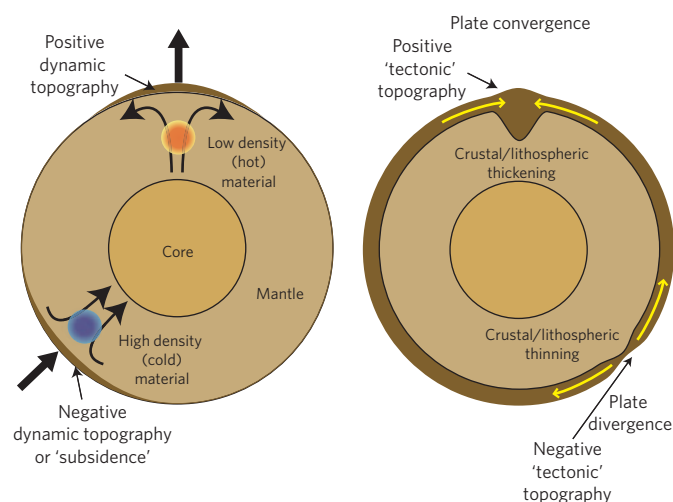


Figure 1 | Dynamic topography. **a**, Simple sketch illustrating how flow in the mantle generates dynamic surface topography. The red and blue circles represent low (hot) and high (cold) density anomalies in the mantle; the black arrows represent the induced mantle flow; resulting dynamic topography is also shown. **b**, Normal, isostatically compensated, tectonic topography is created by thinning or thickening of the crust and lithosphere in response to tectonic plate motions (yellow arrows). Where plates converge, the crust is thickened and mountains (or positive topography) are created; where plates diverge, the crust is thinned and a basin forms. Note that the deflections of the surface and crust are highly exaggerated in both diagrams. Real Earth topography is only a few kilometres high, which is very small in comparison to its 6,700 km radius.

overlying flat subduction systems^{11–14}. Above more steeply dipping slabs, subsidence resulting from the induced mantle corner flow is narrowly focused and affects trench depth and geometry^{12,15}. The realization that mantle plumes are an important contributor to mantle dynamics led to the study and characterization of the dynamic topography associated with the impingement of a plume head^{16,17} and large upwellings or superplumes¹⁸ at the base of the lithosphere. In recent years, mantle flow has also been called on to explain anomalous topography in more unusual settings that involve, for example, the subduction of positively buoyant objects, such as a mid-ocean ridge¹⁹ or the low-density crustal material released from a subducting slab²⁰. The contribution of dynamic topography to local and global apparent sea level and its rate of change has also been the subject of recent work^{10,13,21–24} suggesting that — contrary to what would be expected if the rate of change of topography was primarily controlled by tectonics — it may be impossible to find a stable continental platform that could be used to define a eustatic sea-level curve over any extended time period.

Evidence for dynamic topography in the geological record

One of the first pieces of evidence that mantle flow contributes to surface uplift or subsidence comes from the sedimentary record of western North America where the extent (over a 1,000 km) and gentle tilt of Late Cretaceous sequences could not be explained by tectonic processes¹¹. Similar observations and interpretation were made for parts of the sedimentary record in various basins of eastern Australia^{14,25,26}, the Russian Platform²⁷ and southern Africa²⁸. The now widely accepted interpretation for the existence of these poorly preserved thin wedges of sediment is that they are the remnant of a sequence deposited during the transient tilting of continental interiors, or so-called flooding events, driven by mantle circulation above shallowly dipping subduction zones^{11,29,30}.

Similarly, well-documented episodes of uplift in continental interiors, away from any active plate boundary, have been interpreted as

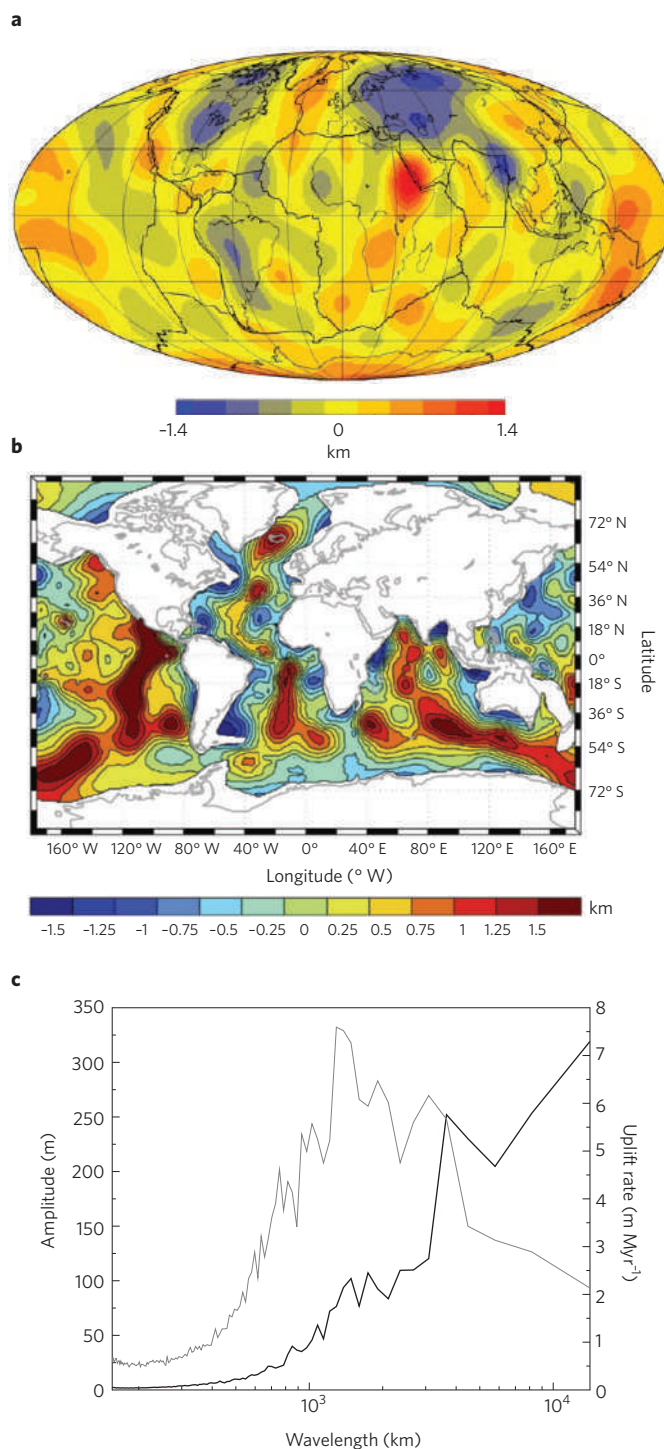


Figure 2 | Estimates of present-day dynamic topography. **a**, Observed dynamic or 'residual' topography as computed by removing the isostatically compensated, tectonically driven component of surface topography. **b**, Dynamic topography as computed by a numerical model of mantle convection driven by density anomalies derived from seismic tomography images. **c**, Distribution of computed dynamic topography and its rate of change, as a function of wavelength (R. Moucha, personal communication). Parts **a** and **b** reproduced with permission from: **a**, ref. 6, © 2007 Elsevier; **b**, ref. 10, © 2008 Elsevier.

related to large-scale upwelling in the underlying mantle. Again, it is the scale (>1,000 km) and rate of uplift that has led geologists to believe that mantle flow is the driving mechanism². However,

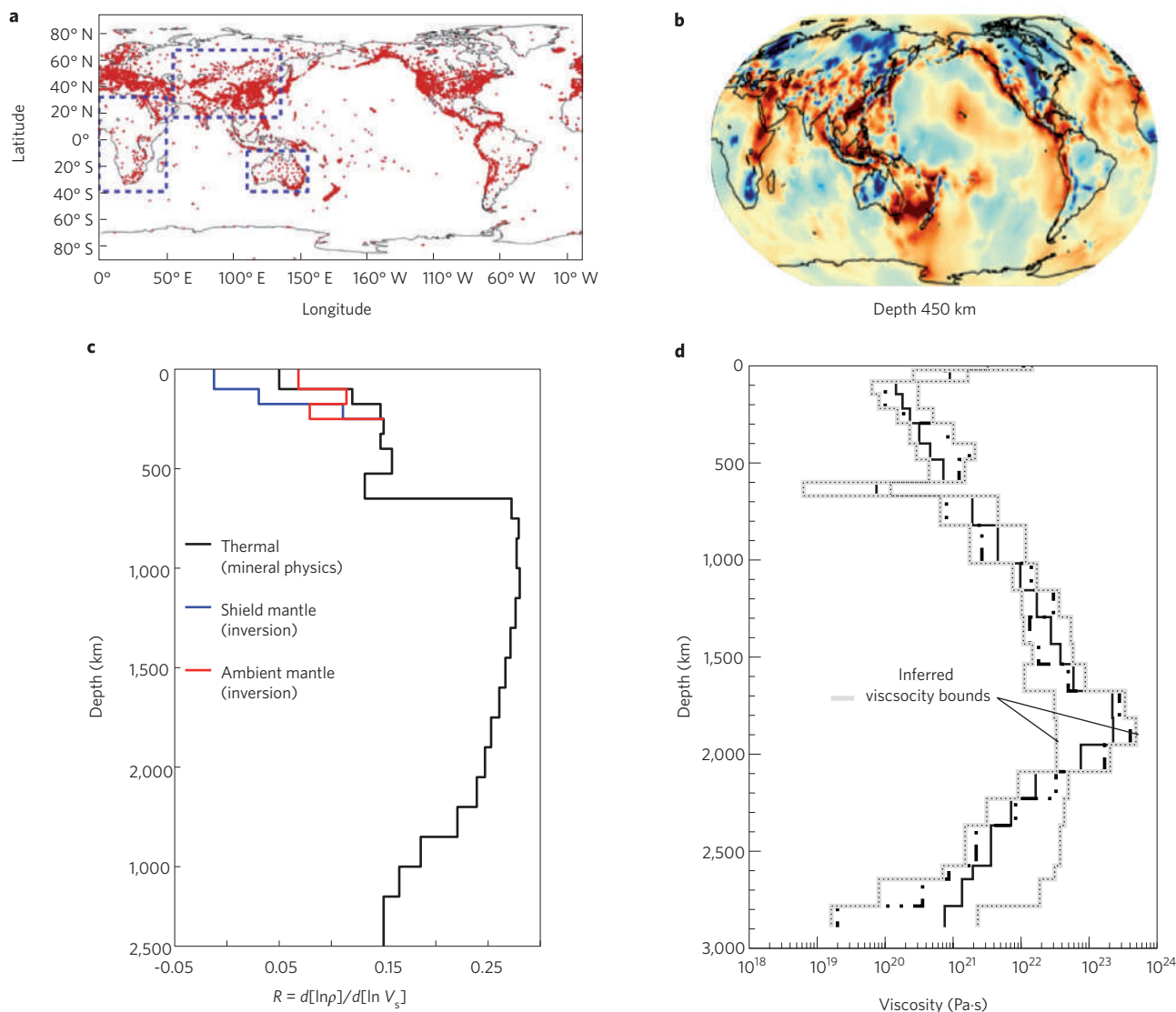


Figure 3 | Components needed to compute past dynamic topography. **a**, Recent seismic station network recording large, distant earthquakes. Red dots correspond to seismic recording stations used to construct a global three-dimensional seismic image of the mantle as shown in **b**. The colour indicates the speed of seismic waves, blue is fast, red is slow. **c**, Example of the complex relationship between rock density (ρ) and seismic shear wave speed (V_s) as a function of depth, used to convert seismic tomography maps into density anomaly maps and drive mantle convection models, where R is the scaling between seismic velocity heterogeneity and density perturbations; for a discussion on the range of possible value for these parameters see refs 52, 56. **d**, Example of a radial viscosity profile used in numerical convection models. Figures reproduced with permission from: **a,b**, ref. 47, © 2008 Elsevier; **c**, ref. 55, © 2007 AGU; **d**, ref. 56, © 2007 Elsevier.

the timing of uplift is generally difficult to constrain from the geological record; it is the resulting erosion that is more accurately documented, mostly through thermochronology, which records the cooling associated with rock exhumation or the resulting sedimentary flux stored in adjacent, non-uplifting areas³¹. One of the most widely cited examples of past (and present?) dynamic topography is the Late Cretaceous rise of the south African craton^{1,18}, the timing of which is still strongly debated: for some³², the pulse-like character of the concomitant sedimentary flux into adjacent margins suggests a process that must be lithospheric in origin.

In the sedimentary record, evidence for past dynamic topography may also take the form of unconformities, where tectonically driven subsidence was perturbed by the dynamical effect of upward mantle flow^{9,33–37} or that of an abnormally thick sedimentary sequence in the case of enhanced subsidence driven by downward mantle flow³⁸. Other observational evidence for dynamic uplift or subsidence is varied and includes the drowning of coral reefs³⁹, volcanism and

its relationship to present-day or past anomalous topography^{3,40}, or current and past states of stress⁴¹. Some have pointed out that the relationship between mantle flow and the associated dynamic uplift may be more complex than currently predicted by simple convection models, owing to either the non-linear response of the lithosphere¹⁷ or to the complex interactions of rising plumes and downgoing slabs with the 660-km discontinuity⁴². Others have also demonstrated that small mantle density anomalies that cannot be evidenced by global seismic tomography may generate an unexpectedly short wavelength component to dynamic topography^{9,23,43}, with the consequence that its expression in the geological record may be confused with effects arising from tectonic events.

Advances in predicting past and present dynamic topography

In recent years, geodynamicists have embarked on a complex modelling exercise to predict past dynamic topography by running mantle convection models backwards in time⁴⁴. In a recent example⁴⁵,

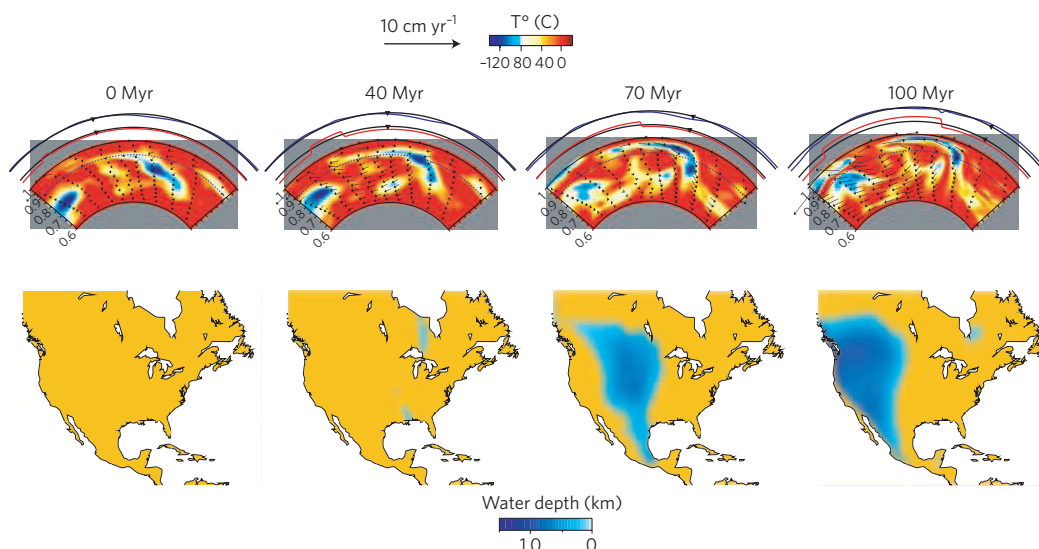


Figure 4 | The advection of present-day mantle-flow models backwards in time. Results of a numerical convection model (achieved following the steps illustrated in Fig. 3) showing computed temperature and velocity fields beneath North America (top panels), as well as the evolving dynamic topography over the past 100 Myr (bottom panels). In the top panels, the blue curve shows the model-predicted dynamic topography along the cross-section shown in the bottom panels; the red curve shows the predicted horizontal surface velocity (or plate motion) along the cross-section. Reproduced with permission from ref. 29, © 2009 AGU.

patterns of mantle flow associated with subduction of the Farallon plate beneath the North American plate are reconstructed back to 100 Myr ago and, based on the model predictions, are used to explain enigmatic parts of the geological record. Four steps are required in this procedure:

- **A three-dimensional map of present-day seismic velocity in the Earth's mantle.** Following improvements in seismic networks and instrumentation, new global seismic datasets have been assembled^{46,47} and complemented by the deployment of temporary arrays⁴⁸ to improve coverage in specific areas. The current resolution of the resulting tomographic models (or three-dimensional pictures of seismic velocity of the Earth's mantle — see ref. 49 for a recent account on past and modern seismic tomography methods) is of the order of a few hundred kilometres for most of the Earth's mantle⁴⁷ (Fig. 3a,b), but still remains variable, with large areas beneath the central Pacific Ocean, the Indian Ocean or Antarctica lacking resolution (>500 km). In contrast, structures in subduction systems or regions characterized by a high seismic-network density, such as in California or Japan, are known with a much better resolution (<100 km). The resolution of the models is also affected by the complex and highly variable structure of the lithosphere, mostly beneath continental areas, and the geometry of the crust–mantle interface that is characterized by a strong contrast in seismic velocity and is traversed by all seismic waves observed at the surface.
- **A physical model to translate these seismic velocity anomalies into density anomalies.** Much work has also been devoted to better understanding the nature of the seismic anomalies we detect in the mantle, that is whether they correspond to temperature or compositional anomalies^{50,51}, and to estimate the corresponding density contrast that mantle dynamicists must use to drive their convection models⁵² (Fig. 3c). This exercise remains approximate, as illustrated by the current debate on the density contrast associated with the lower-mantle seismic anomaly beneath southern Africa^{53–55} that is clearly evidenced in all tomographic models.
- **The mantle viscosity structure.** To compute mantle-flow pattern and intensity from the seismically derived density

distribution, geodynamicists need a good knowledge of rock viscosity within the Earth's mantle. Several models exist that all attempt to explain a wide variety of geophysical observations at a range of spatial and temporal scales⁵⁶ (Fig. 3d). However, no clear consensus has yet emerged, especially for mantle viscosity values near the base of the lithosphere or near the lower mantle–upper mantle boundary, which control the degree of coupling between mantle flow and the overlying lithospheric plates, and the degree to which surface dynamic topography is sensitive to lower-mantle density heterogeneities, respectively. Current models also include lateral viscosity variations^{57,58}, which may become important to properly predict the patterns of mantle flow in subduction systems, for example, where strong lateral temperature and thus viscosity variations exist.

- **An efficient and accurate method to advect present-day mantle-flow models backwards in time.** Computing past dynamic topography requires mantle convection models to be run backwards in time and, concomitantly, to advect the density and temperature fields derived from seismic tomographic models (Fig. 4e,f). Several methods — including so-called adjoint models where one searches for the best initial condition of a forward model that will match the present-day situation — have been recently devised to achieve this^{29,40,44,59} over periods extending back to several tens of millions of years. The most challenging problem arises from the irreversible nature of heat conduction, which mostly affects the accuracy and stability of the various methods within the upper and lower thermal boundary layers (the lithosphere or along the core–mantle boundary).

For the reasons given above, the reconstruction of dynamic topography, even over recent geological times, remains a relatively imprecise exercise as recently demonstrated by the conflicting conclusions on the timing of uplift of the Colorado Plateau derived from two separate models^{40,60}.

Dynamic topography and surface processes

The concept of a dynamic contribution to surface topography has also been embraced by geomorphologists, who now argue that

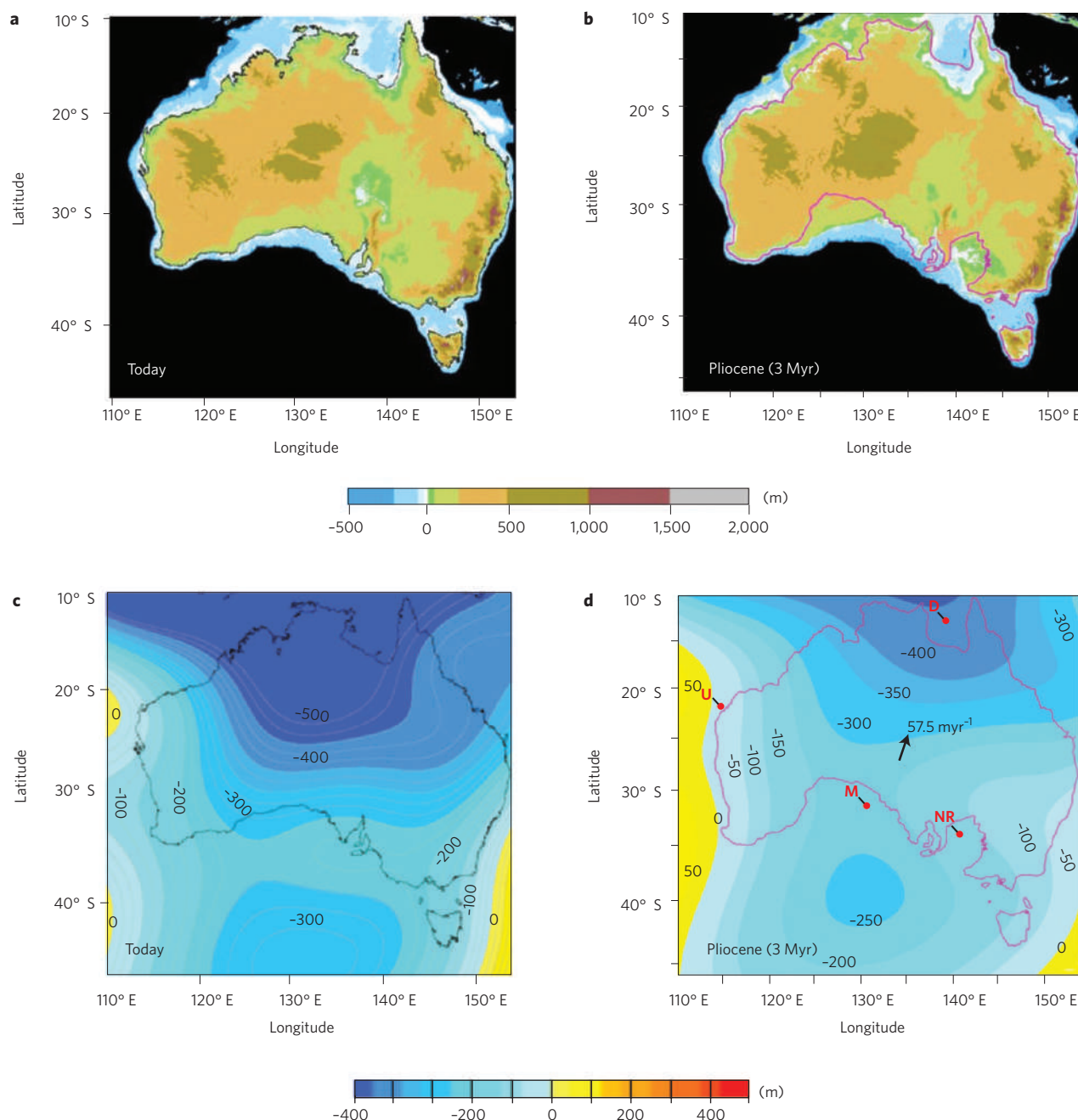


Figure 5 | Example of computed dynamic topography and its comparison to the geological record. Computed palaeogeographic maps (**a,b**) and corresponding dynamic topography (**c,d**) beneath Australia³⁰, shown in a system of reference where Australia is fixed in its present-day position. The contours of dynamic topography (in metres) illustrate the rapid northward motion of the Australian plate relative to a large mantle downwelling that is responsible for the apparent sea-level variations along most of the continental margins. Magenta line corresponds to Pliocene palaeo-shoreline⁷². Red dots and labels correspond to the locations of wells used to constrain the model. Reproduced with permission from ref. 30, © 2010 Elsevier.

evidence for past dynamic topography and its evolution through time will be best recorded in low-relief areas, where the small amplitude and long wavelength surface uplift or subsidence associated with mantle-flow-driven surface topography may cause important and measurable perturbations to drainage networks and catchment geometry, as well as palaeo-shorelines. Recently, predictions of a backward-advected mantle-flow model (as described above) suggest that well-documented geomorphic events such as the Miocene rapid shoreline migration and the change in flow direction and drainage-basin geometry of the palaeo Amazon River may be due to the evolving dynamic topography associated with

the subduction of past (Phoenix and Farallon) and present (Nazca) plates beneath the South American continent^{61,62}. Comparisons of drainage-basin geometry with the position of the seismic-velocity anomaly beneath the Yellowstone region, indicate that the anomalous position of the present-day drainage divide of the Snake River may be due to the eastward migration of the Yellowstone hotspot⁶³, as also indicated by detrital zircon provenance data⁶⁴. The uplift, base-level drop and nickpoint migration associated with the recent (Pliocene?) incision of the Grand Canyon have also been linked to the presence of a slow-seismic-velocity anomaly in the underlying mantle⁶⁵. However, to obtain an accurate picture of the uplift

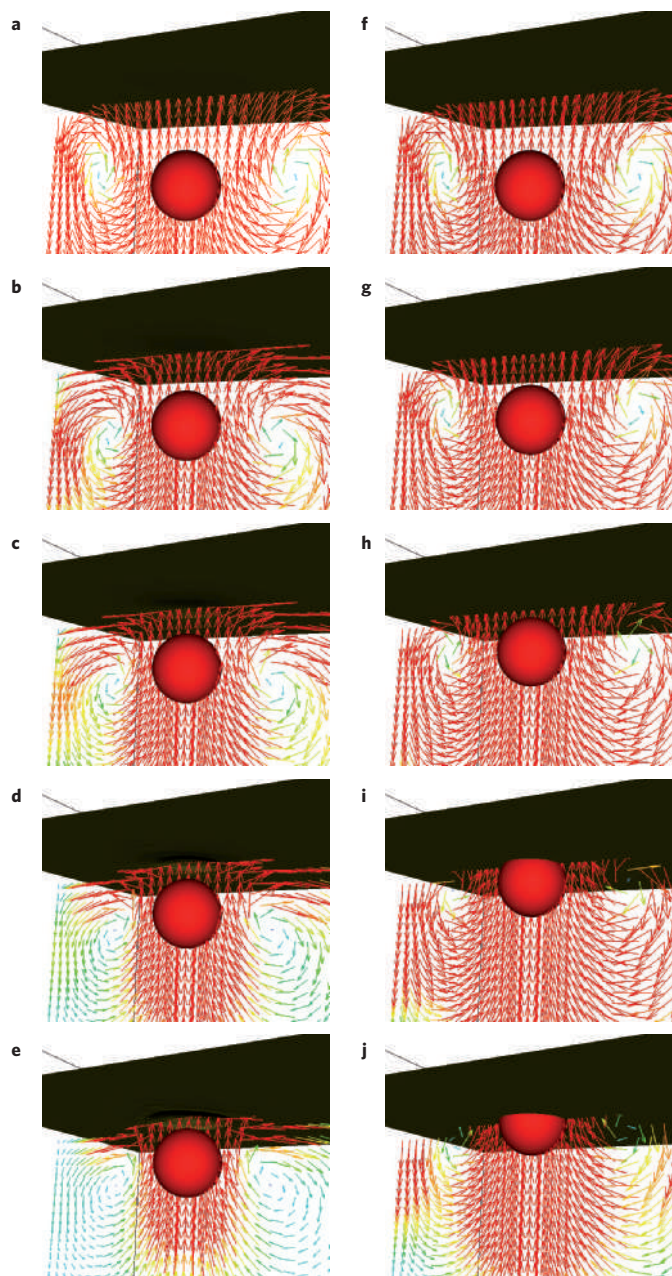


Figure 6 | How eroding dynamic topography can affect mantle flow.

Results of a three-dimensional viscous-flow numerical model illustrating the importance of how surface processes can accelerate flow in an isoviscous mantle. The time steps at which the results are shown are identical in the two experiments. In the first simulation, where surface processes are turned off (panels **a–e**), the rigid, light sphere rises almost twice as slowly as in the second simulation (panels **f–j**) where surface processes are sufficiently efficient to erode dynamic topography at the rate it is being created by mantle flow. See supplementary information for animations of these simulations.

history of this area, one must take into account the rapid westward motion of the North American plate with respect to the underlying mantle⁴⁰. Linking mantle-flow models with plate-reconstruction models is essential for deriving accurate estimates of past dynamic topography and is now routinely done (for example, refs 29,41). In areas where absolute plate motion is fast relative to the mantle, for example the Australian continent (Fig. 5), this may lead to local

changes in dynamic topography and potential local reversals in slope, on a million-year timescale, which is much smaller than the timescale commonly associated with changes in mantle flow.

Along relatively flat continental margins, small changes in surface slope may lead to very large lateral excursions in apparent sea level that are recorded in the evolving geography of palaeo-shorelines. These have commonly been interpreted as related to global or eustatic sea-level changes, but strong evidence now suggests that local mantle flow may be responsible for the observed surface tilt. For example, by mapping marine terraces, changes in surface tilt can be correlated with the migration of a topographic bulge caused by subduction of the Chile Triple Junction beneath the South American craton and the associated upward mantle flow¹⁹. Furthermore, the current asymmetry in coastal morphology between the southern and northern margins of the Australian continent, as well as the presence of Palaeogene palaeo-shorelines along the southern coast of Victoria (southeastern Australia), have been interpreted as resulting from the northward motion of the craton above a deep-seated mantle anomaly⁶⁶. Because of its relative tectonic quiescence since its separation from Antarctica in the Late Cretaceous, the Australian continent is indeed an ideal natural laboratory for studying the effect of mantle dynamics on surface topography and shoreline evolution. Dynamic topography caused by migration of the continent over material subducted along its eastern margin in the Cretaceous and its northern margin in the Oligocene, can explain most of the anomalous subsidence observed in the northern, southern and eastern marginal basins and the associated shoreline evolution^{14,30} (Fig. 5). The well-documented drowned reefs of northeastern Australia have also been linked to the late Miocene episode of enhanced subsidence associated with subduction-driven mantle flow north of Papua New Guinea³⁹.

Erosion and sedimentation effects on mantle flow

Another important question has been at the heart of a long debate in the Earth sciences community: are surface processes (erosion and sedimentation) efficient enough to alter the Earth's dynamics and the rate or amplitude of its internal motion? There is now ample evidence that a feedback exists between erosion and crustal tectonics⁶⁷; but whether this also applies to mantle flow⁶⁸ remains debated.

Dynamic topography generates gravitational stresses that are equal and opposite in sign to the radial viscous stresses resulting from the divergent nature of mantle flow in the vicinity of the Earth's surface. But mantle flow is itself driven by gravitational forces arising from the presence of density variations within the mantle. One can therefore consider that dynamic topography is the expression of a balance between gravitational stresses caused by internal versus surface density variations, and that the viscous mantle provides the coupling. Thus, in this situation, surface processes (erosion/deposition) may become active players in the system by affecting one of the two balancing stresses, and, as shown in the following example, amplify flow in the mantle. Here I present the results of two simple numerical experiments that show a light, rigid sphere moving towards the surface at a rate that is determined by its buoyancy and the viscosity of the fluid (Fig. 6). The two experiments differ by the efficiency of the surface processes: in the first experiment, erosion is turned off, whereas in the second experiment, erosion and sedimentation are assumed to be so efficient so that no dynamic topography ever develops. The effect of the surface processes is drastic: the sphere moves almost twice as fast in the second experiment. Another simple way of understanding the physics of this effect is to consider the predicted velocity field near the surface: in the first experiment, it is strongly divergent and causes high viscous stresses for which work has to be extracted from the rising sphere, whereas in the second

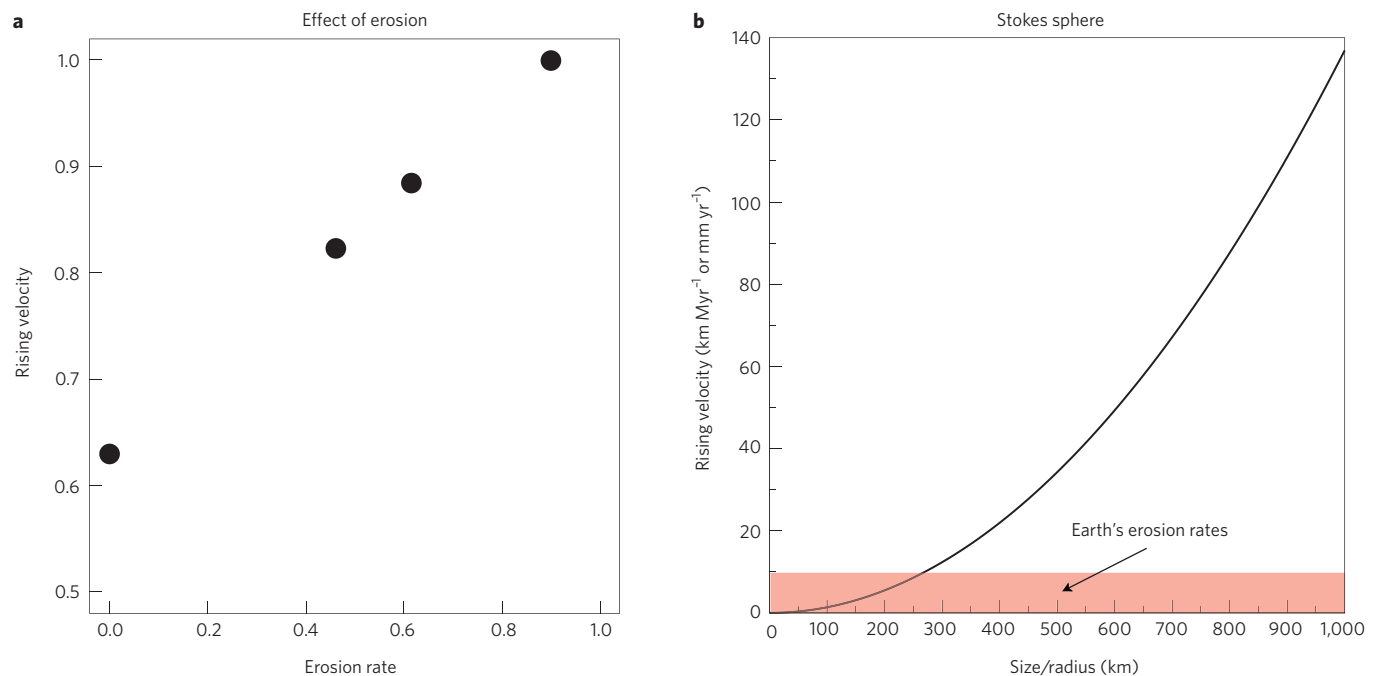


Figure 7 | Earth's erosion rate compared with mantle anomalies' rising velocity. a, Sphere rising velocity versus imposed erosion rate (both normalized by the maximum rising velocity, that is measured in the full erosion experiment) as obtained in four separate numerical experiments, similar to those shown in Fig. 6. The rising velocity is the maximum value achieved by the sphere during the experiment. **b**, Rate of rise of a light sphere rising in the Earth's mantle, as a function of its radius. The Stokes velocity $V_{\text{Stokes}} = 2/9((\Delta\rho g a^2)/\eta)$ of an object is the rate at which a light, rigid sphere of equivalent volume rises in a viscous fluid, which depends only on its radius, a , the density contrast between the sphere and the fluid, $\Delta\rho$, the acceleration due to gravity, g , and the fluid viscosity, η . I have assumed a mean mantle viscosity of 5×10^{21} Pa·s and a density anomaly of 10 kg m^{-3} , based on our best estimates of these values for the Earth's mantle as shown in Fig. 3b,c,d.

experiment, the velocity field is almost unaffected by the presence of the surface, generating greatly reduced, if any, stresses.

The question arises then whether Earth's surface processes are efficient enough to accelerate mantle dynamics. One can easily show (Fig. 7a) that, for dynamic topography to be erased by surface processes, erosion rate needs to be equal to the rising velocity of the sphere. Using the Stokes sphere velocity, one can derive the necessary erosion rate as a function of length scale (Fig. 7b). The range of rates at which surface processes operate on Earth is also indicated. This simple calculation shows that surface processes are too slow to produce a significant feedback on mantle flow at length scales larger than 100–200 km. Adding the strong viscosity contrast between the mantle and the lithosphere also greatly dampens this effect. Although the simplicity of the calculations presented here should not prevent future work on the subject, it seems quite unlikely that surface processes have any significant effect on large-scale mantle-flow dynamics. These results suggest, however, that the motion of small, anomalously dense/light bodies — such as a pluton rising through the Earth's crust — could be strongly affected by erosional processes. Furthermore, the non-linear nature of the Earth's rheology results in a substantial proportion of the mantle energy being dissipated at plate boundaries⁶⁹ where large topographic gradients exist and thus erosional processes are very efficient. This, in turn, may imply that plate motions, and thus mantle flow, are to some extent controlled by surface processes⁶⁸.

Mantle flow should also generate kilometre-scale dynamic topography at the core–mantle boundary¹. The strong hydromagnetic coupling that is likely to exist along this boundary may lead to efficient erosion of any topography of that surface, that is on a very short timescale, suggesting that mantle flow near the base of the mantle where strong plume-like features are generated may be strongly influenced by the efficiency of erosion of mantle topography in the core⁷⁰.

Dynamic topography as a new constraint on mantle flow

Mantle dynamics remain poorly constrained, but by linking mantle flow to surface topography, and the evolution of this dynamic topography through time, we obtain a means of using the geological record to constrain the dynamics and viscosity of the mantle and the density structure that controls its flow. Unlike tomographic images, which only offer snapshots of present-day mantle structure, the study of dynamic topography offers insights into the past dynamics of the mantle. The effects of dynamic topography are stored in the geological record, albeit in an incomplete fashion, owing to the transient nature of the topography. For geophysicists, this will drive further research towards the development of sophisticated methods to invert the present-day mantle structure (for example, ref. 69) by running the mantle flow backwards in time. For geologists, the challenge will lie in deciphering the complex and imperfectly preserved record of slowly changing, small-amplitude surface motion that results from mantle flow. This is most promising in regions not recently affected by tectonic events, such as the African or Australian continents. Linking mantle flow with the geological record will require new large-scale surface-process models that accurately calculate patterns of erosion, reorganizations of drainage systems and sedimentary fluxes that result from the broad, low-amplitude dynamic topography (for example, ref. 71). The goal would be to directly invert geological observations to constrain the Earth's mantle dynamics through time.

References

1. Hager, B., Clayton, C., Richards, M., Comer, R. & Dziewonski, A. Lower mantle heterogeneity, dynamic topography and the geoid. *Nature* **313**, 541–545 (1985).
2. Gurnis, M., Mitrovica, J., Ritsema, J. & van Heijst, H.-J. Constraining mantle density structure using geological evidence of surface uplift rates: The case of the African superplume. *Geochem. Geophys. Geosyst.* **1**, 1020 (2000).
3. Lowry, A., Ribe, N. & Smith, R. Dynamic elevation of the Cordillera, western United States. *J. Geophys. Res.* **105**, 23371–23390 (2000).

4. Conrad, C., Lithgow-Bertelloni, C. & Loudon, K. Iceland, the Farallon slab, and dynamic topography of the North Atlantic. *Geology* **32**, 177–180 (2004).
5. Guillou-Frotier, L., Burrov, E., Nehlig, P. & Wyns, R. Deciphering plume–lithosphere interactions beneath Europe from topographic signatures. *Glob. Planet. Change* **58**, 119–140 (2007).
6. Steinberger, B. Effects of latent heat release at phase boundaries on flow in the Earth's mantle, phase boundary topography and dynamic topography at the Earth's surface. *Phys. Earth Planet. Inter.* **164**, 2–20 (2007).
7. Adam, C. & Vidal, V. Mantle flow drives the subsidence of oceanic plates. *Science* **328**, 83–85 (2010).
8. Hillier, J. Subsidence of normal seafloor: observations do indicate flattening. *J. Geophys. Res.* **115**, B03102 (2010).
9. Winterbourne, J., Crossby, A. & White, N. Depth, age and dynamic topography of oceanic lithosphere beneath heavily sedimented Atlantic margins. *Earth Planet. Sci. Lett.* **287**, 137–151 (2009).
10. Moucha, R. *et al.* Dynamic topography and long-term sea-level variations: there is no such thing as a stable continental platform. *Earth Planet. Sci. Lett.* **271**, 101–108 (2008).
11. Mitrovica, J., Beaumont, C. & Jarvis, G. Tilting of continental interiors by the dynamical effects of subduction. *Tectonics* **8**, 1079–1094 (1989).
12. Gurnis, M. Phanerozoic marine inundation of continents driven by dynamic topography above subducting slabs. *Nature* **364**, 589–593 (1993).
13. Spasojevic, S., Liu, L., Gurnis, M. & Muller, R. The case for dynamic subsidence of the US east coast since the Eocene. *Geophys. Res. Lett.* **35**, L08305 (2008).
14. DiCaprio, L., Gurnis, M. & Muller, R. Long-wavelength tilting of the Australian continent since the Late Cretaceous. *Earth Planet. Sci. Lett.* **278**, 175–185 (2009).
15. Husson, L. Dynamic topography above retreating subduction zones. *Geology* **34**, 741–744 (2006).
16. Artyushkov, E. & Hofmann, A. Neotectonic crustal uplift on the continents and its possible mechanisms: the case of southern Africa. *Surv. Geophys.* **18**, 369–415 (1998).
17. Burrov, E. & Guillou-Frotier, L. The plume head–continental lithosphere interaction using a tectonically realistic formulation for the lithosphere. *Geophys. J. Int.* **161**, 469–490 (2005).
18. Lithgow-Bertelloni, C. & Silver, P. Dynamic topography, plate driving forces and the African superswell. *Nature* **395**, 269–272 (1998).
19. Guillaume, B., Martinod, J., Husson, L., Roddaz, M. & Riquelme, R. Neogene uplift of central eastern Patagonia: dynamic response to active spreading ridge subduction? *Tectonics* **28**, TC2009 (2009).
20. Sutherland, R., Spasojevic, S. & Gurnis, M. Mantle upwelling after Gondwana disconnection death explains anomalous topography and subsidence histories of eastern New Zealand and West Antarctica. *Geology* **38**, 155–158 (2010).
21. Muller, R., Sdrolias, M., Gaina, C., Steinberger, B. & Heine, C. Long-term sea-level fluctuations driven by ocean basin dynamics. *Science* **319**, 1357–1362 (2008).
22. Conrad, C. & Husson, L. Influence of dynamic topography on sea level and its rate of change. *Lithosphere* **1**, 110–120 (2009).
23. Lovell, B. A pulse in the planet: regional control of high-frequency changes in relative sea level by mantle convection. *J. Geol. Soc. Lond.* **167**, 637–648 (2010).
24. Petersen, K., Nielsen, S., Clausen, O., Stephenson, R. & Gerya, T. Small-scale mantle convection produces stratigraphic sequences in sedimentary basins. *Science* **329**, 827–830 (2010).
25. Gallagher, K. & Lambeck, K. Subsidence, sedimentation and sea-level changes in the Eromanga Basin, Australia. *Basin Res.* **2**, 115–131 (1989).
26. Gurnis, M., Muller, R. & Moresi, L. Cretaceous vertical motion of Australia and the Australian Antarctic discordance. *Science* **279**, 1499–1504 (1998).
27. Mitrovica, J., Pysklywec, R. & Beaumont, C. The Devonian to Permian tilting of the Russian platform: an example of subduction controlled long-wavelength tilting of continents. *J. Geodyn.* **22**, 79–96 (1996).
28. Pysklywec, R. & Mitrovica, J. The role of subduction-induced subsidence in the evolution of the Karoo Basin. *J. Geol.* **107**, 155–164 (1999).
29. Spasojevic, S., Liu, L. & Gurnis, M. Adjoint models of mantle convection with seismic, plate motion, and stratigraphic constraints: North America since the Late Cretaceous. *Geochem. Geophys. Geosyst.* **10**, Q05W02 (2009).
30. Heine, C., Muller, R., Steinberger, B. & DiCaprio, L. Integrating deep Earth dynamics in paleogeographic reconstructions of Australia. *Tectonophysics* **483**, 135–150 (2010).
31. Gallagher, K. & Brown, R. The onshore record of passive margin evolution. *J. Geol. Soc. Lond.* **154**, 451–457 (1997).
32. Gallagher, K. & Brown, R. In *The Oil and Gas Habitats of the South Atlantic* (eds Cameron, N., Bate, R. & Clure, V.) 41–53 (Geological Society of London Special Publication Vol. 153, 1999).
33. Walford, H. & White, N. Constraining uplift and denudation of west African continental margin by inversion of stacking velocity data. *J. Geophys. Res.* **110**, B04403 (2005).
34. Al-Hajri, Y., White, N. & Fishwick, S. Scales of transient convective support beneath Africa. *Geology* **37**, 883–886 (2009).
35. Rudge, J., Shaw Champion, M., White, N., McKenzie, D. & Lovell, J. A plume model of transient diachronous uplift at the Earth's surface. *Earth Planet. Sci. Lett.* **267**, 146–160 (2008).
36. Shaw Champion, M., White, N., Jones, S. & Lovell, J. Quantifying transient mantle convective uplift: an example from the Faroe–Shetland basin. *Tectonics* **27**, TC1002 (2008).
37. Heine, C., Muller, R., Steinberger, B. & Torsvik, T. Subsidence in intracontinental basins due to dynamic topography. *Phys. Earth Planet. Inter.* **171**, 252–264 (2008).
38. Downey, N. & Gurnis, M. Instantaneous dynamics of the cratonic Congo basin. *J. Geophys. Res.* **114**, B06401 (2009).
39. DiCaprio, L., Muller, R. & Gurnis, M. A dynamic process for drowning carbonate reefs on the northeastern Australian margin. *Geology* **38**, 11–14 (2010).
40. Moucha, R. *et al.* Deep mantle forces and the uplift of the Colorado Plateau. *Geophys. Res. Lett.* **36**, L19310 (2009).
41. Forte, A., Moucha, R., Simmons, N., Grand, S. & Mitrovica, J. Deep-mantle contributions to the surface dynamics of the North American continent. *Tectonophysics* **481**, 3–15 (2010).
42. Leng, W. & Zhong, S. Surface subsidence caused by mantle plumes and volcanic loading in large igneous provinces. *Earth Planet. Sci. Lett.* **291**, 207–214 (2010).
43. Le Pourhiet, L., Gurnis, M. & Saleeby, J. Mantle instability beneath the Sierra Nevada Mountains in California and Death Valley extension. *Earth Planet. Sci. Lett.* **251**, 104–119 (2006).
44. Conrad, C. & Gurnis, M. Seismic tomography, surface uplift, and the breakup of Gondwanaland: Integrating mantle convection backwards in time. *Geochem. Geophys. Geosyst.* **4**, 1031 (2003).
45. Liu, L., Spasojevic, S. & Gurnis, M. Reconstructing Farallon plate subduction beneath North America back to the Late Cretaceous. *Science* **322**, 934–938 (2008).
46. Grand, S. Mantle shear-wave tomography and the fate of subducted slabs. *Phil. Trans. R. Soc. Lond. A* **360**, 2475–2491 (2002).
47. Li, C., van der Hilst, R., Engdahl, E. & Burdick, S. A new global model for P wave speed variations in Earth's mantle. *Geochem. Geophys. Geosyst.* **9**, Q05018 (2008).
48. Burdick, S. *et al.* Model update December 2008: upper mantle heterogeneity beneath North America from P-wave travel time tomography with global and USArray transportable array data. *Seismol. Res. Lett.* **80**, 638–645 (2008).
49. Rawlinson, N., Pozgay, S. & Fishwick, S. Seismic tomography: a window into deep Earth. *Phys. Earth Planet. Inter.* **178**, 101–135 (2009).
50. Karato, S.-I. & Karki, B. Origin of lateral variation of seismic wave velocities and density in the deep mantle. *J. Geophys. Res.* **106**, 21771–21784 (2001).
51. Stixrude, L. & Lithgow-Bertelloni, C. Thermodynamics of mantle minerals. Part 1: Physical properties. *Geophys. J. Int.* **162**, 610–632 (2005).
52. Simmons, N., Forte, A. & Grand, S. Joint seismic, geodynamic and mineral physical constraints on three-dimensional mantle heterogeneity: implications for the relative importance of thermal versus compositional heterogeneity. *Geophys. J. Int.* **177**, 1284–1304 (2009).
53. Ni, S., Tan, E., Gurnis, M. & Helmberger, D. Sharp sides to the African superplume. *Science* **296**, 1850–1852 (2002).
54. Behn, M., Conrad, C. & Silver, P. Detection of upper mantle flow associated with the African superplume. *Earth Planet. Sci. Lett.* **224**, 259–274 (2004).
55. Simmons, N., Forte, A. & Grand, S. Thermomechanical structure and dynamics of the African super-plume. *Geophys. Res. Lett.* **34**, L02301 (2007).
56. Forte, A. in *Treatise of Geophysics* (eds Romanovitch, B. & Dziewonski, A.) 805–854 (GEOTOP Publication Vol. 1, 2007).
57. Tan, E., Choi, E., Thoutireddy, P., Gurnis, M. & Aivazis, M. Geoframework: coupling multiple models of mantle convection within a computational framework. *Geochem. Geophys. Geosyst.* **7**, Q06001 (2006).
58. Moucha, R., Forte, A., Mitrovica, J. & Daradich, A. Lateral variations in mantle rheology: implications for convection related surface observables and inferred viscosity models. *Geophys. J. Int.* **169**, 113–135 (2007).
59. Bunge, H.-P., Hagelberg, C. & Travis, B. Mantle circulation models with variational data assimilation: Inferring past mantle flow and structure from plate motion histories and seismic tomography. *Geophys. J. Int.* **152**, 280–301 (2003).
60. Liu, L. & Gurnis, M. Dynamic subsidence and uplift of the Colorado Plateau. *Geology* **38**, 663–666 (2010).
61. Shephard, G. E., Muller, R. D., Liu, L. & Gurnis, M. Miocene drainage reversal of the Amazon River driven by plate–mantle interaction. *Nature Geosci.* **3**, 870–875 (2010).
62. Shephard, G. *et al.* Contribution of mantle convection to shifting South American coastlines during the Tertiary. *Eos* **90**, 52 (2009).
63. Wegmann, K. *et al.* Position of the Snake River watershed divide as an indicator of geodynamic processes in the greater Yellowstone region, western North America. *Geosphere* **3**, 272–281 (2007).
64. Beranek, L., Link, P. & Fanning, C. Miocene to Holocene landscape evolution of the western Snake River plain region, Idaho: using the SHRIMP detrital zircon provenance record to track eastward migration of the Yellowstone hotspot. *Geol. Soc. Am. Bull.* **118**, 1027–1050 (2006).

65. Karlstrom, K., Crow, R., Crossey, L., Coblentz, D. & van Wijk, J. Model for tectonically driven incision of the younger than 6 Ma Grand Canyon. *Geology* **36**, 835–838 (2008).
66. Sandiford, M. The tilting continent: a new constraint on the dynamic topographic field from Australia. *Earth Planet. Sci. Lett.* **261**, 152–163 (2007).
67. Finnegan, N. *et al.* Coupling of rock uplift and river incision in the Namche Barwa-Gyala Peri Massif, Tibet. *Geol. Soc. Am. Bull.* **120**, 142–155 (2008).
68. Iaffaldano, G. & Bunge, H.-P. Strong plate coupling along the Nazca–South America convergent margin. *Geology* **36**, 443–446 (2008).
69. Stadler, G. *et al.* The dynamics of plate tectonics and mantle flow: from local to global scales. *Science* **329**, 1033–1038 (2010).
70. Jault, D. & Le Moul, J.-L. Core–mantle boundary shape: constraints inferred from the pressure torque acting between the core and the mantle. *Geophys. J. Int.* **101**, 233–241 (2007).
71. Simoes, M., Braun, J. & Bonnet, S. Continental-scale erosion and transport laws: A new approach to quantitatively investigate macroscale landscapes and associated sediment fluxes over the geological past. *Geochem. Geophys. Geosyst.* **11**, Q09001 (2010).
72. Langford, R., Wilford, G., Truswell, E. & Isern, A. *Paleogeographic Atlas of Australia: Cainozoic* (Australian Geological Survey Organization, 1995).

Acknowledgements

The author wishes to thank S. Braun, T. Gerya and B. Steinberger for constructive comments on an earlier version of this manuscript.

Additional information

Supplementary information accompanies this paper on www.nature.com/naturegeoscience.